



Luminophore-immobilized mesoporous silica for selective Hg^{2+} sensing

Min Hee Lee,^a Soo Jin Lee,^b Jong Hwa Jung,^{b,*} Heungbin Lim^a and Jong Seung Kim^{c,*}

^aDepartment of Chemistry, Dankook University, Seoul 140-714, Republic of Korea

^bDepartment of Chemistry and Research Institute of Natural Science, Gyeongsang National University, Jinju 660-701, Republic of Korea

^cDepartment of Chemistry, Korea University, Seoul 136-701, Republic of Korea

Received 18 July 2007; revised 14 August 2007; accepted 20 August 2007

Available online 5 September 2007

Abstract—Novel mesoporous silica-immobilized rhodamine (**MSIR**) and silica particle-immobilized rhodamine (**SPIR**) anchored by a tren ($\text{N}(\text{CH}_2\text{CH}_2\text{NH}_2)_3$) were synthesized. The binding and adsorption abilities of both **MSIR** and **SPIR** for metal cations were investigated with fluorophotometry and ion chromatography, respectively. Both **MSIR** and **SPIR** show selectivity for Hg^{2+} ion over other metal cations because the Hg^{2+} ion selectively induces a ring opening of the rhodamine fluorophores. The sensitivity of the **MSIR** for Hg^{2+} ion is greater than that of the **SPIR** and the **MSIR** adsorbs 70% of Hg^{2+} ion while the **SPIR** does only 40%. The **MSIR** can be also easily recovered by treatment of a solution of TBA^+OH^- . For the application of Hg^{2+} detection in the environmental field, the **MSIR**-coated glass plate is also developed and exhibits an excellent function in visual and fluorescence changes with Hg^{2+} ion.

© 2007 Elsevier Ltd. All rights reserved.

1. Introduction

Fluorescent molecules for transition and heavy metal cation sensors such as Hg^{2+} , Cu^{2+} , Pb^{2+} , and Zn^{2+} ions have been increasingly important as tools for the quantitative and the qualitative monitoring of the target metal ions in many biological and environmental processes.^{1–8} Then, based upon the concepts of the host–guest chemistry, cation sensing has recently risen to a dominant position in research devoted to the detection of designated species. An effective fluorescence chemosensor must convert the event of cation recognition by the ionophore into an easily monitored and highly sensitive light signal from the fluorophore.^{9,10} As such a fluorogenic unit, rhodamine dyes have been used for conjugation with biomolecules for fluorescent probes^{11–16} owing to their excellent fluorescence properties. A spirolactam form of rhodamine is generally non-fluorescent and colorless. By the addition of guest ions to a solution of the rhodamine, however, the rhodamine shows a strong fluorescence and a pink color.

Recently, the use of organic–inorganic materials has been interesting in the research for new methodologies for ion recognition and sensing. The receptor-immobilized inorganic

materials such as SiO_2 , Al_2O_3 , and TiO_2 have some important advantages^{17–25} as a solid chemosensor in heterogeneous solid-liquid phase. First, immobilized receptor on the inorganic support can liberate the organic guest molecule (metal and anion ions) to the solution of the pollutant.

Second, the organic–inorganic hybrid nanomaterials can be recyclable by suitable chemical treatment. Lastly, functionalized nanomaterials combined with fluorophore or chromophore display high selective and sensitive fluorescence or absorption changes because of their large surface area and well-defined pores in comparison to spherical structures. So, taking advantage of the homogeneous porosity with the large surface area, the mesoporous silica as an inorganic support has been quite interesting.^{26–34}

Most receptor-immobilized inorganic materials developed so far have been known to be related to their UV band changes upon metal ion introduction. For example, Nazeeruddin et al. reported colorimetric, fluorimetric, and electrochemical detection of mercury ions by functionalized ruthenium sensitizers in aqueous and non-aqueous solutions, on anchored TiO_2 films, but the most concern would be the colorimetric Hg^{2+} sensing.^{6,8}

In this context, we have developed a mesoporous silica-immobilized rhodamine (**MSIR**) because of its significant fluorescence change as well as color variation in the event

Keywords: Rhodamine; Mercury sensing; Mesoporous silica.

* Corresponding authors. E-mail addresses: jonghwa@gnu.ac.kr; jongskim@korea.ac.kr

of the Hg^{2+} ion-induced spirolactam ring opening. Hence, we now report its adsorption ability along with fluorescence responses upon the addition of various metal cations.

2. Results and discussion

The **MSIR** was prepared by coupling reaction of **1** and mesoporous silica in toluene. Compound **1** was synthesized by condensation of rhodamine-tren **2** with 3-(triethoxysilyl)propylisocyanate in toluene as a solvent. The mesoporous silica was prepared by adaptation of synthetic methods published earlier.^{21,22} For the comparison of the functional advantages of the **MSIR**, the commercial silica-bounded rhodamine was also prepared via similar synthetic route to **MSIR** (Schemes 1 and 2).

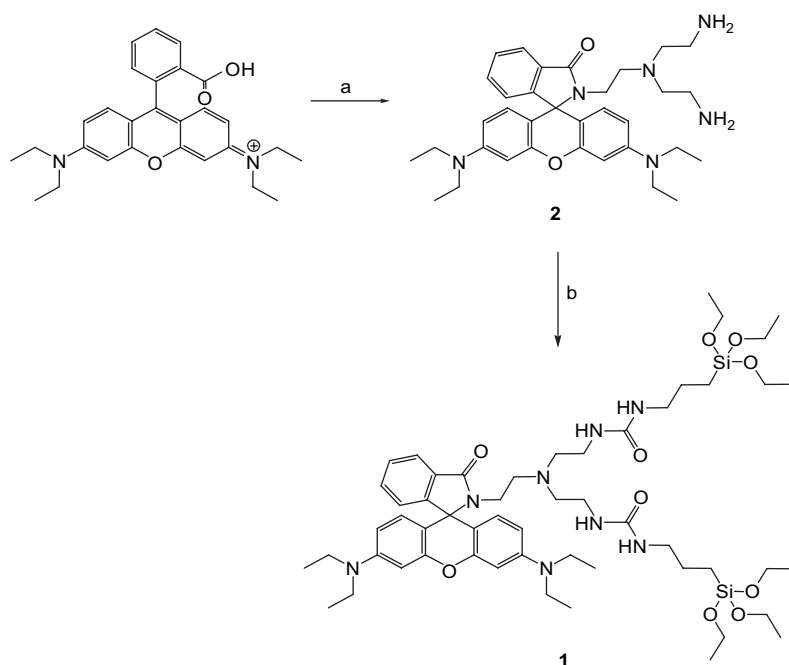
The synthetic **MSIR** was well characterized by transmission electron microscopy (TEM), thermogravimetric analysis (TGA), energy dispersive X-ray spectroscopy (EDX), FTIR spectroscopy (IR), and fluorophotometry.

In Figure 1, the TEM pictures clearly show the formation of well-ordered hexagonal arrangement of mesoporous

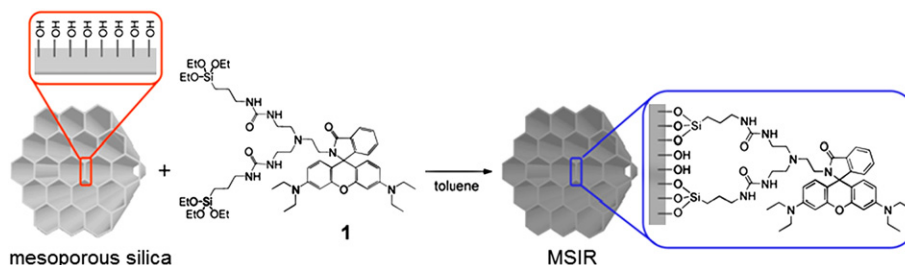
channels before and after attaching **1** with which the mesoporous silica still retains a well-ordered hexagonal arrangement.

To gain insight into the porosity changes of the mesoporous silica induced by the introduction of **1**, we measured the surface area, pore volumes, and pore diameters of both mesoporous silica and **MSIR** with nitrogen adsorption–desorption isotherms. Figure S1 shows the nitrogen adsorption–desorption isotherms and Barrett–Joyner–Halenda (BJH) pore diameters of the periodic mesoporous silica and **MSIR**. The mesoporous silica has a BET (Brunauer–Emmett–Teller)^{35,36} surface area of 1119.72 m²/g and a pore volume of 0.49 cm³/g. On the other hand, we observed that fluorescent **MSIR** has a BET surface area of 377.21 m²/g and a pore volume of 0.26 cm³/g (Fig. S1A). The mesoporous silica and the **MSIR** have BJH pore diameters of 2.246 and 2.155 nm, respectively (Fig. S1B). The decreased surface area and pore diameter in **MSIR** are attributable to the attachment of rhodamine to the mesoporous silica.

For the comparison of the porosity effect and the binding ability of the **MSIR** with those of the commercial silica,



Scheme 1. Synthetic routes to **1** and **2**. Conditions: (a) tris(2-aminoethyl)amine, MeOH, 80 °C and (b) 3-(triethoxysilyl)propylisocyanate, toluene, 80 °C.



Scheme 2. Synthetic method of **MSIR**.

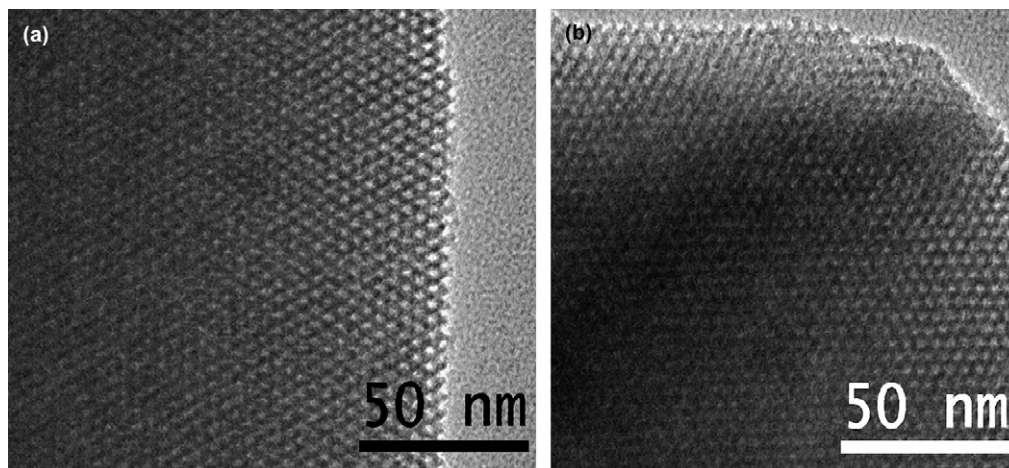


Figure 1. TEM images of mesoporous silica (a) and MSIR (b).

we have also prepared silica particle-immobilized rhodamine (**SPIR**) from the reaction of **1** with the commercial silica. From the results of TGA experiment (Fig. 2), we noticed that the **SPIR** consists of only 8.1 wt % of **1** whereas the **MSIR** has 23.1 wt %, obviously because the commercial silica particle has much smaller surface area (510.00 m²/g) than the mesoporous silica (1119.72 m²/g).

Besides, for further structural proof of the **MSIR**, we carried out IR spectroscopy of both mesoporous silica and **MSIR**, in which the mesoporous silica appears at 3450, 1658, and 1084 cm⁻¹ whereas the **MSIR** does at 3382, 2975, 2948, 1656, 1634, 1614, 1517, and 1084 cm⁻¹ (Figs. S2 and S3). The new peaks of 2975, 2948, 1656, 1634, 1614, and 1517 cm⁻¹ are originated from the rhodamine, giving us a solid evidence that **1** is certainly attached onto the surface of the mesoporous silica. Moreover, the strong fluorescence emission of the **MSIR** with an excitation at 520 nm definitely arises from the introduction of **1** to the mesoporous silica (vide infra). In addition, EDX measurements indicate that **MSIR** contains nitrogen (N) and carbon (C) atoms, which do not exist in the mesoporous silica (Fig. S4),

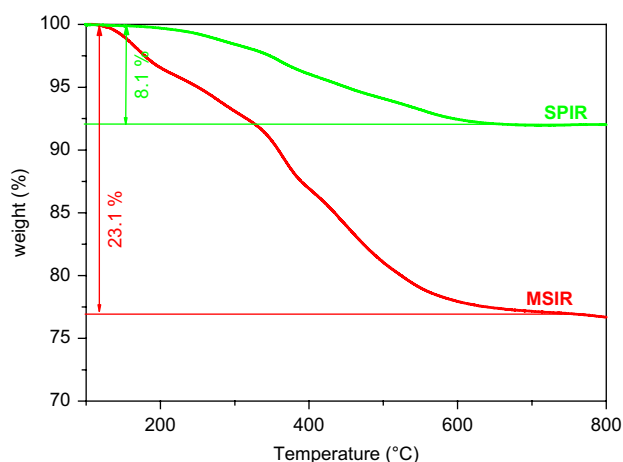


Figure 2. Thermogravimetric analysis data of **MSIR** (red) and **SPIR** (green).

supporting a clear fact that **1** covalently attaches onto the surface of mesoporous silica.

Then we investigated spectroscopic properties of the **MSIR** and the **SPIR** toward metal ion complexation. In the absence of specific guest ions, CH₃CN suspension of the **MSIR** is non-fluorescent and colorless because the rhodamine molecule is in a spirolactam form. In the presence of the metal ions, however, the suspension of **MSIR** remarkably shows an enhancing fluorescence emission centered at 588 nm (Fig. 3a) and color change from colorless to pink (Fig. 3b). From these spectroscopic changes, we noticed that the **MSIR** reveals a high selectivity for Hg²⁺ ion over other metal cations. It should be noteworthy that interaction of rhodamine on the surface of **MSIR** with Hg²⁺ ion induces a highly conjugated rhodamine system via formation of opened-spirolactam to give a strong fluorescence emission as well as a pink color. For the **SPIR**, however, we observed same properties of enhancing fluorescence emission and color changes with addition of Hg²⁺ ion as for the **MSIR**, but a rather low sensitivity (see Fig. S5), implicating that the **MSIR** we have developed is considerably applicable to the environmental field.

Additionally, the adsorption abilities of **MSIR** and **SPIR** for metal cations were also estimated by ion chromatography (Fig. 4). We observed that **MSIR** and **SPIR** adsorb 70% and 40% of Hg²⁺ ion, respectively, indicating that the **MSIR** is better adsorbent than the **SPIR** for the separation of Hg²⁺ ion. For other metal cations such as Zn²⁺, Pb²⁺, and Cu²⁺, the **MSIR** showed an adsorption abilities less than 4–11%.

In the aspect of material recovery, the **MSIR**·Hg²⁺ was treated with a solution of tetrabutylammonium hydroxide (TBA⁺OH⁻). Interestingly, we found that the fluorescence of the **MSIR**·Hg²⁺ declines and vanishes by addition of the base as shown in Figure 5. In addition to the fluorescence quenching, the color change from pink to colorless was observed as seen in Figure 3b. With the fluorescence off–on–off upon metal and base treatment, we are sure that the **MSIR** can be recyclable in the environmental usage.

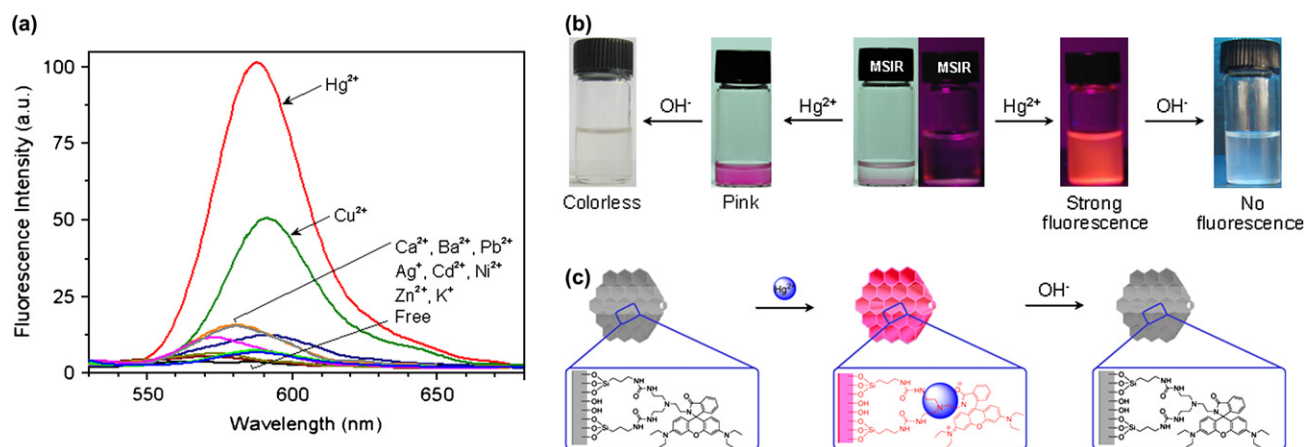


Figure 3. (a) Fluorescence spectra of **MSIR** (0.09 mM) upon addition of ClO_4^- salts of various metal ions (2.25 mM) in CH_3CN with an excitation at 520 nm; (b) visual change (left) and fluorescence change (right) toward to Hg^{2+} and OH^- ions; and (c) Plausible binding mechanism of **MSIR** for Hg^{2+} ion.

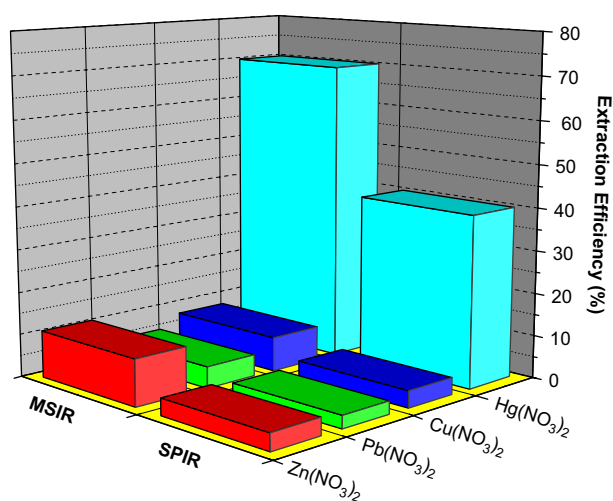


Figure 4. IC chromatograms of metal ions by addition of **MSIR** and **SPIR**.

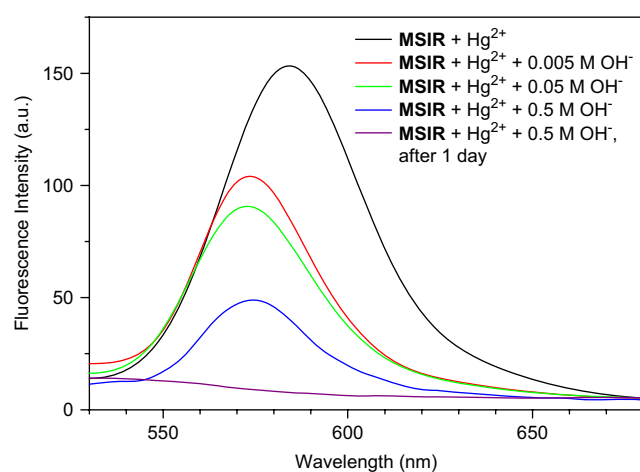


Figure 5. Fluorescence spectra of (0.09 mM) **MSIR** · Hg^{2+} (2.25 mM) upon addition of various amount of tetrabutylammonium hydroxide (TBA^+OH^-) in CH_3CN with an excitation at 520 nm.

What is the nature of the fluorescence change in **MSIR** with Hg^{2+} ion? For this question, we investigated a fluorescence property of **1** upon Hg^{2+} ion complexation. **Figure S6** indicates absorption and fluorescence changes of **1** upon titration of the Hg^{2+} ion. Addition of Hg^{2+} ion induces the spiro-lactam ring of **1** to open to give a new absorption band at 550 nm and enhanced fluorescence intensity at 588 nm.¹³ As a result, one can assert that the fluorescence change of the **MSIR** is originated from the structural change of **1**.

To prove the binding mode of the **MSIR** with Hg^{2+} ion, we first conducted FTIR spectroscopy for both **MSIR** and **MSIR** · Hg^{2+} complex. It was observed that upon the addition of Hg^{2+} ion, the carbonyl ($\text{C}=\text{O}$) stretching band at 1656 cm^{-1} in the spiro-lactam moves to lower wave-number. This confirms that the Hg^{2+} ion is attached to the **MSIR** in which oxygen atom of the rhodamine carbonyl group takes part in the complexation with the Hg^{2+} ion (**Fig. 3c** and **Fig. S3**).

In consideration of extending its usefulness, the **MSIR** was coated in $50\text{ }\mu\text{m}$ thickness onto the glass substrate ($20\text{ mm}\times 50\text{ mm}$). We then observed that the color of **MSIR**-coated glass substrates changes from colorless to pink with Hg^{2+} ion. This result can be applicable to detect the low concentrated Hg^{2+} ion up to $1.0\times 10^{-5}\text{ M}$ by a naked-eye inspection (**Fig. 6**).

3. Conclusions

A novel mesoporous silica-immobilized rhodamine (**MSIR**) targeting for selective response to Hg^{2+} ion over other metal ions is developed. The sensitivity of the **MSIR** for Hg^{2+} ion is greater than that of the **SPIR**. In adsorption ability for Hg^{2+} ion, **MSIR** (70%) is better than **SPIR** (40%). In addition, in the light of portable colorimetric and fluorimetric kit for detection of Hg^{2+} ion in the environmental field, the glass plate-coated **MSIR** is prepared and shows an excellent function in visual and fluorescence changes with Hg^{2+} ion. In addition, the **MSIR** can be easily recovered by treatment of a solution of TBA^+OH^- .

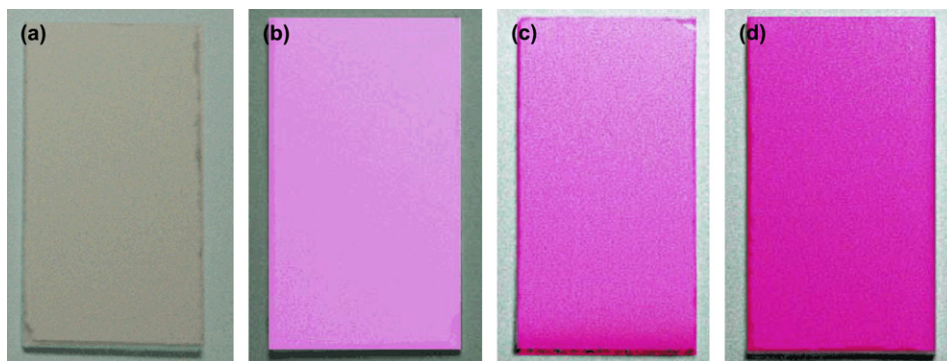


Figure 6. MSIR-coated glass substrate (a) without Hg^{2+} , (b) 1.0×10^{-5} , (c) 1.0×10^{-4} , and (d) 1.0×10^{-3} M.

4. Experimental

4.1. Preparation of MSIR and SPIR

Compound **1** (20 mg, 0.02 mmol) was dissolved in anhydrous toluene (5 mL) to which the mesoporous silica (100 mg) or commercial silica was also added and stirred in reflux condition under N_2 for 24 h. The collected solid was washed several times with methylene chloride and acetone to rinse away any surplus **1**. **MSIR** or **SPIR** was obtained as a solid (100 mg). IR (KBr pellet, cm^{-1}): 3382, 2975, 1656, 1517/3326, 1634, 1554, 1063.

4.2. Preparation of **1**

Compound **2** (160 mg, 0.28 mmol) and 3-(triethoxysilyl)propylisocyanate (0.15 g, 0.62 mmol) were dissolved in toluene (10 mL) and stirred in reflux condition under N_2 for 24 h. After cooling to room temperature, the solvent was evaporated in vacuo. CH_2Cl_2 (100 mL) and water (200 mL) were added, and the organic layer was separated. The CH_2Cl_2 layer was washed twice with water followed by drying over anhydrous Na_2SO_4 . After filtration of sodium sulfate, removal of the solvent in vacuo gave a brownish crude that was further purified by column chromatography on silica gel (ethyl acetate/methanol, 100:1) to provide 150 mg of brownish oil **1** in 50% yield. Compound **1** contains Si–OEt where –OEt is known for a good leaving group, inducing Si-polymerization in the presence of oxygen. So, the immobilization reaction of the Si–OEt to mesoporous silica should be implemented under N_2 . IR (deposit from CH_2Cl_2 solution on a NaCl plate, cm^{-1}): 3346, 2973, 1690, 1079; FABMS m/z (M^+) calcd 1065.5, found 1065.0; ^1H NMR (CDCl_3 , 200 MHz): δ 7.90 (m, 1H), 7.46 (m, 2H), 7.10 (m, 1H), 6.37–6.33 (m, 6H), 6.15 (s, 2H), 5.10 (s, 2H), 3.87–3.77 (q, 12H), 3.36–3.29 (m, 8H), 3.16–3.10 (m, 10H), 2.33 (s, 4H), 1.90 (s, 2H), 1.60 (m, 4H), 1.28–1.13 (q, 30H), 0.70 (t, $J=8.79$ Hz, 4H). ^{13}C NMR (CDCl_3 , 50 MHz): 168.9, 158.7, 158.4, 153.5, 152.6, 148.8, 131.1, 128.7, 108.3, 104.8, 97.5, 66.3, 58.2, 54.2, 44.2, 42.7, 37.5, 23.8, 18.2, 12.4, 7.5 ppm.

4.3. Preparation of **2**

Under nitrogen, a solution of rhodamine B (0.40 g, 0.84 mmol) and tren (0.24 g, 1.68 mmol) in methanol

(20 mL) was heated at 80 °C until the solution appears colorless from pink. After cooling to room temperature, the solvent was evaporated in vacuo. CH_2Cl_2 (100 mL) and water (200 mL) were added, and the organic layer was separated. The CH_2Cl_2 layer was washed twice with water followed by drying over anhydrous Na_2SO_4 . After filtration of sodium sulfate, removal of the solvent in vacuo gave 0.40 g of **2** as colorless oil in 85% yield. IR (deposit from CH_2Cl_2 solution on a NaCl plate, cm^{-1}): 3352, 1683, 1515, 1515; FABMS m/z (M^+) calcd 570.37, found 571.00; ^1H NMR (CDCl_3 , 200 MHz): δ 7.90 (m, 1H), 7.46 (m, 2H), 7.10 (m, 1H), 6.43–6.29 (d, 6H, $J_1=8.8$ Hz, $J_2=5.6$ Hz), 3.39–3.28 (q, 8H), 2.54–2.51 (t, 2H), 2.37–2.21 (m, 6H), 1.60–1.40 (br s, 4H), 1.20–1.13 (t, 12H, $J=6.90$ Hz). ^{13}C NMR (CDCl_3 , 50 MHz): 167.6, 153.4, 148.8, 132.2, 131.6, 128.9, 128.1, 123.7, 122.6, 108.1, 105.6, 97.6, 64.9, 56.8, 44.3, 39.5, 38.1, 12.5 ppm.

4.4. Synthesis of the mesoporous silica

The silica precursor, tetraethyl orthosilicate (TEOS), was added to an aqueous solution of octadecyltrimethylammonium chloride (ODTMA) as a surfactant under a strong acidic condition at room temperature, with the molar ratio of $100\text{H}_2\text{O}/7\text{HCl}/0.02\text{ODTMA}/0.03\text{TEOS}$. The mixture was then stored in the isothermal oven set at 95 °C for 1 day. The mesoporous silica was obtained by collecting the white precipitate that was washed with water several times.

4.5. Adsorption of metal ions by MSIR and SPIR

A CH_3CN solution of metal ion (2.0×10^{-4} mM) with 10 mg of **MSIR** or **SPIR** was stirred for 10 min at room temperature. After filtration, the concentration of metal ions remained in organic phase was analyzed by ion chromatography (DX-500, DIONEX).

4.6. MSIR-coated glass substrate

To 1.0 mL of a solution of H_2O (0.5 mL) and EtOH (0.5 mL), 200 mg of **MSIR** was added and the mixture was shaken for 1 min. Then, the slurry product was spread evenly over a glass surface and was left to dry for approximately 30 min. The final step is to place the product in an oven for 30 min at a maximum temperature of 105 °C.

4.7. Fluorescence investigation

Fluorescence emission and UV–vis spectra were conducted on RF-5301-PC and S-2130 instruments, respectively. Stock solutions (0.01 M) of the hydrated metal perchlorate salts were prepared in CH₃CN. Stock solutions of **MSIR**, **SPIR**, and **1** were prepared in CH₃CN. For all measurements, excitation was 520 nm with excitation and emission slit widths at 1.5 nm.

Acknowledgements

This work was supported by the SRC program (R11-2005-008-02001-0(2006)) and KOSEF (R01-2005-000-10229-0). In addition, this work was partially supported by Korea Ministry of Environments as ‘The Eco-technopia 21 Project’.

Supplementary data

Supplementary data associated with this article can be found in the online version, at doi:10.1016/j.tet.2007.08.113.

References and notes

- Bryan, A. J.; de Silva, A. P.; de Silva, S. A.; Rupasinghe, R. A. D. D.; Sandanayake, K. R. A. S. *Biosensors* **1989**, *4*, 169.
- Woodroffe, C. C.; Lippard, S. J. *J. Am. Chem. Soc.* **2003**, *125*, 11458.
- Kim, S. K.; Lee, S. H.; Lee, J. Y.; Bartsch, R. A.; Kim, J. S. *J. Am. Chem. Soc.* **2004**, *126*, 16499.
- Kim, S. K.; Kim, S. H.; Kim, H. J.; Lee, S. H.; Lee, S. W.; Ko, J.; Bartsch, R. A.; Kim, J. S. *Inorg. Chem.* **2005**, *44*, 7866.
- Lee, S. J.; Jung, J. H.; Seo, J.; Yoon, I.; Park, K.-M.; Lindoy, L. F.; Lee, S. S. *Org. Lett.* **2006**, *8*, 1641.
- Nazeeruddin, M. K.; Di Censo, D.; Humphry-Baker, R.; Grätzel, M. *Adv. Funct. Mater.* **2006**, *16*, 189.
- Métivier, R.; Leray, I.; Lebeau, B.; Valeur, B. *J. Mater. Chem.* **2005**, *15*, 2965.
- Coronado, E.; Galan-Mascaros, J. R.; Marti-Gastaldo, C.; Palomares, E.; Durrant, J. R.; Vilar, R.; Grätzel, M.; Nazeeruddin, M. K. *J. Am. Chem. Soc.* **2005**, *127*, 12351.
- Nohta, H.; Satozono, H.; Koiso, K.; Yoshida, H.; Ishida, J.; Yamaguchi, M. *Anal. Chem.* **2000**, *72*, 4199.
- Okamoto, A.; Ichiba, T.; Saito, I. *J. Am. Chem. Soc.* **2004**, *126*, 8364.
- Dujols, V.; Ford, F.; Czarnik, A. W. *J. Am. Chem. Soc.* **1997**, *119*, 7386.
- John, G.; Mason, M.; Ajayan, P. M.; Dordick, J. S. *J. Am. Chem. Soc.* **2004**, *126*, 15012.
- Yang, Y.-K.; Yook, K.-J.; Tae, J. *J. Am. Chem. Soc.* **2005**, *127*, 16760.
- Xiang, Y.; Tong, A. *Org. Lett.* **2006**, *8*, 1549.
- Albers, A. E.; Okreglak, V. S.; Chang, C. J. *J. Am. Chem. Soc.* **2006**, *128*, 9640.
- Zheng, H.; Qian, Z.-H.; Xu, L.; Yuan, F.-F.; Lan, L.-D.; Xu, J.-G. *Org. Lett.* **2006**, *8*, 859.
- Wight, A. P.; Davis, M. E. *Chem. Rev.* **2002**, *102*, 3589.
- Topoglidis, E.; Campbell, C. J.; Palomares, E.; Durrant, J. R. *Chem. Commun.* **2002**, 1518.
- Lai, C.-Y.; Trewyn, B. G.; Jeftinija, D. M.; Jeftinija, K.; Xu, S.; Jeftinija, S.; Lin, V. S.-Y. *J. Am. Chem. Soc.* **2003**, *125*, 4451.
- Numata, M.; Li, C.; Bae, A.-H.; Kaneko, K.; Sakurai, K.; Shinkai, S. *Chem. Commun.* **2005**, 4655.
- Lee, S. J.; Lee, S. S.; Lah, M. S.; Hong, J.-M.; Jung, J. H. *Chem. Commun.* **2006**, 4539.
- Lee, S. J.; Lee, S. S.; Lee, J. Y.; Jung, J. H. *Chem. Mater.* **2006**, *18*, 4713.
- Son, S. J.; Lee, S. B. *J. Am. Chem. Soc.* **2006**, *128*, 15974.
- Palomares, E.; Vilar, R.; Green, A.; Durrant, J. R. *Adv. Funct. Mater.* **2004**, *14*, 111.
- Balaji, T.; El-Safty, S. A.; Matsunaga, H.; Hanaoka, T.; Mizukami, F. *Angew. Chem., Int. Ed.* **2006**, *45*, 7202.
- Kresge, C. T.; Leonowicz, M. E.; Roth, W. J.; Vartuli, J. C.; Beck, J. S. *Nature* **1992**, *359*, 710.
- Yang, H.; Coombs, N.; Ozin, G. A. *Nature* **1997**, *386*, 692.
- Zhao, D.; Feng, J.; Huo, Q.; Melosh, N.; Fredrickson, G. H.; Chmelka, B. F.; Stucky, G. D. *Science* **1998**, *279*, 548.
- Sakamoto, Y.; Kaneda, M.; Terasaki, O.; Zhao, D. Y.; Kim, J. M.; Stucky, G.; Ryoo, R. *Nature* **2000**, *408*, 449.
- Kim, J. M.; Stucky, G. D. *Chem. Commun.* **2000**, 1159.
- Kleitiz, F.; Marlow, F.; Stucky, G. D.; Schuth, F. *Chem. Mater.* **2001**, *13*, 3587.
- Wong, M. S.; Cha, J. N.; Choi, K.-S.; Deming, T. J.; Stucky, G. D. *Nano Lett.* **2002**, *2*, 583.
- Kruk, M.; Asefa, T.; Jaroniec, M.; Ozin, G. A. *J. Am. Chem. Soc.* **2002**, *124*, 6383.
- Mamak, M.; Metraux, G. S.; Petrov, S.; Coombs, N.; Ozin, G. A.; Green, M. A. *J. Am. Chem. Soc.* **2003**, *125*, 5161.
- Brunauer, S.; Emmett, P. H.; Teller, E. *J. Am. Chem. Soc.* **1938**, *60*, 309.
- Banerjee, I. A.; Yu, L.; Matsui, H. *Proc. Natl. Acad. Sci. U.S.A.* **2003**, *100*, 14678.